

# Electronic Structure of High-Spin Iron(IV) Complexes

Abhik Ghosh,<sup>\*,[a]</sup> Espen Tangen,<sup>[a]</sup> Hege Ryeng,<sup>[a]</sup> and Peter R. Taylor<sup>\*,[b]</sup>

**Keywords:** High-spin species / Nonheme / Iron / Oxo ligand / Diamond core / Quantum chemistry

High-spin ( $S = 2$ ) iron(IV) species are rare but increasingly recognized as reactive intermediates in the catalytic cycles of several nonheme iron enzymes. A question of some interest, therefore, concerns how much higher in energy the low-spin ( $S = 1$ ) state is for these species. With the use of density functional theory (DFT) and high-level ab initio calculations [CASPT2 and CCSD(T)], we have attempted to answer this question for the so-called Collins complex, a square-pyramidal  $\text{Fe}^{\text{IV}}$  complex with a tetraamido-*N* equatorial ligand set, a chloride axial ligand, and an  $S = 2$  ground state. The calculations suggest that relative to the ground state, the low-spin state is higher in energy by at least 0.3 eV and possibly as much as 0.7 eV. Using DFT calculations, a broad quantum chemical survey of high-spin  $\text{Fe}^{\text{IV}}\text{O}$  intermediates was also undertaken. A key finding is that the Fe–O distance and O spin population are quite similar across all mononuclear  $\text{Fe}^{\text{IV}}\text{O}$  species studied, regardless of the heme versus non-

heme environment and of the  $S = 1$  versus 2 spin state, reflecting the essential similarity of the  $\text{Fe}(\text{d}_{\pi})\text{--O}(\text{p}_{\pi})$  orbital interactions in all the species studied. However, the spin density profiles of high-spin  $\text{Fe}^{\text{IV}}\text{O}$  species, currently believed to be known only as a nonheme iron enzyme (TauD) intermediate, are predicted to be very different from that of Collins' high-spin  $\text{Fe}^{\text{IV}}$  complex. Our calculations further suggest that with the help of sterically hindered ligands such as 6-me<sub>3</sub>-tpa, it might be possible to generate synthetic high-spin  $\text{Fe}^{\text{IV}}\text{O}$  models of the unique TauD intermediate. Finally, our calculations confirm the aptness of describing the  $[(6\text{-me}_3\text{-tpa})\text{Fe}^{\text{III}}(\mu\text{-O})_2\text{Fe}^{\text{IV}}(6\text{-me}_3\text{-tpa})]^{3+}$  cation as a flexible diamond core and indicate the presence of a fairly discrete high-spin  $\text{Fe}^{\text{IV}}\text{O}$  unit within the dinuclear core.

(© Wiley-VCH Verlag GmbH & Co. KGaA, 69451 Weinheim, Germany, 2004)

## Introduction

Although high-spin iron(IV) species are believed to be involved in the catalytic cycles of a number of nonheme iron enzymes,<sup>[1,2]</sup> they are exceedingly rare in a traditional inorganic context. This is not surprising given that high oxidation states are generally favored by strongly basic ligands, which in turn normally favor low-spin states of the coordinated transition metal ion. Indeed, a square-pyramidal  $\text{Fe}^{\text{IV}}$  complex with a macrocyclic tetraamido-*N* equatorial ligand and a chloride axial ligand, reported by Collins and co-workers more than a decade ago, serves as the only well-characterized high-spin  $\text{Fe}^{\text{IV}}$  species known.<sup>[3]</sup> At least three enzymatic high-spin  $\text{Fe}^{\text{IV}}$  species have been spectroscopically characterized but until now they have not lent themselves to X-ray crystallographic analysis. Perhaps the most celebrated example of a high-spin  $\text{Fe}^{\text{IV}}$  species is the critical

methane-hydroxylating intermediate **Q** of sMMO.<sup>[4]</sup> There is strong evidence indicating that **Q** features an  $[\text{Fe}^{\text{IV}}_2(\mu\text{-O})_2]^{4+}$  diamond core with antiferromagnetically coupled local high-spin  $\text{Fe}^{\text{IV}}$  centers.<sup>[2,4]</sup> A related  $\text{Fe}^{\text{III}}\text{Fe}^{\text{IV}}$  species called intermediate **X** produces the catalytically essential tyrosyl radical in the R2 protein of ribonucleotide reductase to initiate the process of ribonucleotide reduction in DNA biosynthesis.<sup>[5]</sup> On the modeling front, Que and co-workers have reported synthetic  $[\text{Fe}_2(\mu\text{-O})_2]^{3+}$  intermediates with localized high-spin  $\text{Fe}^{\text{III}}$  and  $\text{Fe}^{\text{IV}}$  centers, the high-spin character of the metal centers reflecting the relatively weak-field nature of the capping ligands, which are based on sterically hindered 2,6-dialkylpyridine units.<sup>[6,7]</sup> Finally and very recently, a high-spin  $\text{Fe}^{\text{IV}}$  intermediate of the mononuclear nonheme iron enzyme TauD (taurine/ $\alpha$ -ketoglutarate dioxygenase) has been spectroscopically detected.<sup>[8]</sup> Given our longstanding interest in the electronic structures of high-valent transition metal species,<sup>[9]</sup> we have initiated a broad quantum chemical exploration of the electronic structures of various known high-spin  $\text{Fe}^{\text{IV}}$  species, this being our first report on the subject.

We present our results in two parts. In the first part, we present our efforts to model the well-characterized Collins species mentioned above,<sup>[3]</sup> focusing on benchmarking the relative energies of the high- and low-spin states using density functional theory (DFT) and ab initio CASPT2 and

<sup>[a]</sup> Department of Chemistry, University of Tromsø, 9037 Tromsø, Norway  
Fax: (internat.) + 47-77644765  
E-mail: abhik@chem.uit.no

<sup>[b]</sup> Department of Chemistry, University of Warwick, Coventry, UK  
Fax: (internat.) + 44-2476-523258  
E-mail: p.r.taylor@warwick.ac.uk

Supporting information for this article is available on the WWW under <http://www.eurjic.org> or from the author.

CCSD(T) calculations.<sup>[10]</sup> The results emphasize the difficulty of the problem – an issue that is largely overlooked in modern quantum chemical studies of bioinorganic problems – but that said, the DFT results are not bad at all, and DFT is clearly indicated as the method of choice for a broad survey of high-spin Fe<sup>IV</sup> species. In the second part of this paper, we present such a survey, focusing on high-spin Fe<sup>IVO</sup> species, including a model of the TauD intermediate.

## The Collins Complex

Before undertaking a broad quantum chemical survey of high-spin Fe<sup>IVO</sup> species, it seemed worthwhile to obtain a feel for the suitability of DFT for such a study. While DFT has emerged as the almost universal method of choice for bioinorganic modeling studies, a number of cases have been documented in which DFT apparently does a poor job of describing the relative energetics of the low-lying states of transition metal complexes.<sup>[10]</sup> Indeed, based on the somewhat limited data available, Fe<sup>III</sup> complexes appear to be particularly problematic; for example, DFT (PW91, B3LYP) does not exhibit a clear preference for a sextet ground state for (porphyrin)Fe<sup>III</sup> chloride, as expected on the basis of experimental data, whereas CASPT2 and CCSD(T) calculations clearly yield the correct ground state and a substantial sextet-quartet splitting of about 0.7 eV.<sup>[11]</sup> In a recent review article,<sup>[10]</sup> we have summarized much of what has been accomplished so far in terms of benchmarking the energetics of key spin states of transition metal species of bioinorganic relevance. As the only well-characterized high-spin Fe<sup>IV</sup> complex, the Collins complex appeared to be an ideal candidate for our benchmarking studies.

To address the essence of the benchmarking problem, there seemed little to be gained by dealing with the relatively complex macrocyclic tetraamido-*N* ligand used in the experimental study.<sup>[3]</sup> We have therefore used the smaller *C*<sub>2v</sub> model complex **1** shown in Figure 1, which captures the key structural features of the synthetic complex.<sup>[3]</sup> Geometry optimizations were carried out for the *S* = 1 and 2 states of the model complex with both the PW91 and B3LYP functionals.<sup>[12]</sup> CASPT2 and CCSD(T) calculations<sup>[13]</sup> were carried out at both the PW91 and B3LYP optimized geometries. The CASPT2 calculations were car-

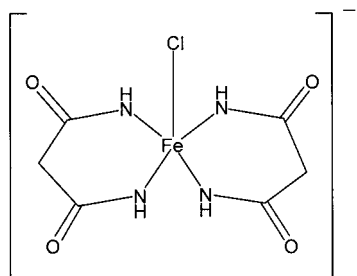


Figure 1. Simplified *C*<sub>2v</sub> model **1** of the complex used in this study

ried out with two high-quality basis sets, denoted BS1 and BS2, the latter being significantly larger than the former.<sup>[14]</sup> Basis set BS1 was used for the CCSD(T) calculations. Table 1 lists selected geometry parameters for the PW91 and B3LYP structures as well as the PW91 Mulliken spin populations for selected atoms.<sup>[15,16]</sup> The agreement between the optimized and experimental<sup>[3]</sup> geometry parameters may be regarded as generally very good.<sup>[15]</sup> The triplet-quintet splitting turned out to be essentially zero with the PW91 functional and 0.21 eV (with the triplet higher in energy) with B3LYP DFT calculations, which clearly emphasized the need for benchmarking with more elaborate, correlated methods such as CASPT2 and CCSD(T).

Table 1. Selected geometry parameters (Å, °) and Mulliken spin populations<sup>[15]</sup>

	<i>S</i> = 1		<i>S</i> = 2	
	PW91	B3LYP	PW91	B3LYP
Geometry parameters <sup>[a][b]</sup>				
Fe–N	1.893	1.896	1.927	1.925
Fe–Cl	2.164	2.198	2.331	2.349
Fe–N <sub>4</sub>	0.343	0.345	0.372	0.376
N–Fe–Cl	100.44	100.48	101.12	101.25
Mulliken spin populations <sup>[c]</sup>				
Fe	1.632		3.149	
N	0.043		0.074	
Cl	0.059		0.330	
C(CO)	0.002		–0.003	
O(CO)	0.036		0.050	

<sup>[a]</sup> In general, the PW91 and B3LYP geometry parameters are in excellent agreement, better than ±0.01 Å and ±0.05°. The only exception is the Fe–Cl distance, for which a somewhat larger difference is observed between the two functionals. <sup>[b]</sup> The symbol Fe–N<sub>4</sub> refers to the distance of the Fe atom from the plane containing the four nitrogen atoms. <sup>[c]</sup> The version of Turbomole used for the B3LYP optimizations does not report atomic spin populations.

At the CASPT2/BS1 level and with B3LYP optimized geometries, the triplet-quintet splitting was found to be 0.66 eV, or 0.56 eV if Fe 3s3p correlation was excluded. With the larger basis set BS2 and B3LYP geometries, the CASPT2 triplet-quintet splitting was 0.69 eV, or 0.58 eV if Fe 3s3p correlation was excluded. CCSD(T) calculations including 3s3p correlation were too large for our computational resources: the triplet-quintet splitting at the CCSD(T)/BS1 level without Fe 3s3p correlation, with B3LYP optimized geometries, was found to be 0.26 eV. Thus, agreement between the CASPT2 and CCSD(T) energetics is only fair, with a difference of about 0.3 eV between the two predictions when Fe 3s3p correlation is excluded. This discrepancy is as large as the splitting itself predicted by DFT [or by CCSD(T)] and begs the question as to which results (if any) are to be relied on.<sup>[17]</sup> On a more positive note, the triplet-quintet splitting obtained with B3LYP energetics is not bad and essentially the same as the CCSD(T) result, indicating the suitability of DFT for a broader exploration of high-spin Fe<sup>IV</sup> intermediates; we have indeed carried out such a study and the results are outlined below.

## High-Spin Fe<sup>IV</sup>O Intermediates

A question of longstanding interest concerns the possible involvement of Fe<sup>IV</sup>O intermediates in the catalytic cycles of *mononuclear* nonheme iron enzymes such as the pterin-dependent enzyme phenylalanine hydroxylase and the  $\alpha$ -ketoglutarate-dependent enzyme prolyl hydroxylase.<sup>[1]</sup> However, as mentioned above, only very recently has the first such species been spectroscopically characterized: this is an intermediate of the mononuclear nonheme iron enzyme TauD (taurine/ $\alpha$ -ketoglutarate dioxygenase), for which Mössbauer spectroscopic studies suggest a unique high-spin Fe<sup>IV</sup> formulation.<sup>[8]</sup> While the ligation state of the iron center is not known, mechanistic considerations suggest that this may be an Fe<sup>IV</sup>O species, which would make it the first *mononuclear* high-spin Fe<sup>IV</sup>O intermediate – enzymatic or synthetic – to be spectroscopically characterized.

Considerable progress has also been made on the synthetic modeling front. Thus, the groups of Wieghardt<sup>[18]</sup> and Que<sup>[19,20]</sup> have synthesized and spectroscopically characterized a number of mononuclear nonheme Fe<sup>IV</sup>O intermediates.<sup>[1]</sup> One of these intermediates, Fe<sup>IV</sup>(O)(me<sub>4</sub>cyclam)(CH<sub>3</sub>CN), has also lent itself to a high-quality crystallographic analysis.<sup>[21]</sup> However, none of these species, which are  $S = 1$ , faithfully mimic the  $S = 2$  TauD intermediate. In contrast, a formally dinuclear but “flexible” diamond-core intermediate formulated as [(6-me<sub>3</sub>-tpa)Fe<sup>III</sup>–O–Fe<sup>IV</sup>(6-me<sub>3</sub>-tpa)=O]<sup>3+</sup> and containing anti-ferromagnetically coupled, localized high-spin Fe<sup>III</sup> and Fe<sup>IV</sup> centers, reported by Que and co-workers, may provide the closest synthetic mimic of a mononuclear  $S = 2$  Fe<sup>IV</sup>O intermediate.<sup>[22]</sup> Given the well-documented ability of sterically hindered 6-alkylated tpa ligands to enforce high-spin states of coordinated Fe<sup>III</sup> and Fe<sup>IV</sup> ions,<sup>[23,24]</sup> it is natural to consider (6-me<sub>3</sub>-tpa)Fe<sup>IV</sup>(O)(L) (where L is an, as yet, undefined ligand) species as attractive synthetic models for the  $S = 2$  TauD intermediate. We have done so in this study, and indeed a high-spin ground state appears likely for such species. Also presented are the first results of our attempts to model the flexible diamond core mentioned above.

The optimized structures of the  $S = 1$  species Fe<sup>IV</sup>-(O)(L)<sub>2</sub>(PhCN) (**2**: L = en; **3**: L = tmen) and of Fe<sup>IV</sup>-(O)(P)(PhCN) (**4**), shown in Figure 2, provide a comparison of the electronic character of the Fe<sup>IV</sup>O unit in heme with nonheme environments.<sup>[25]</sup> Figure 2 shows that for a particular *trans* ligand (PhCN in all these cases), the Fe–O bond lengths are nearly identical in all three species and very similar to that observed experimentally for Fe<sup>IV</sup>(O)-(me<sub>4</sub>cyclam)(CH<sub>3</sub>CN).<sup>[21]</sup> As long known for (porphyrin)Fe<sup>IV</sup>O derivatives (peroxidase compound II analogues),<sup>[26,27]</sup> the electron spin density is almost completely localized on the FeO unit for all three species **2–4** and also partitioned rather similarly between the Fe and O atoms.

The TauD iron site has a 2-His-1-carboxylate ligand environment,<sup>[8]</sup> which we have chosen to model with chelating bis(2-imidazolyl)methane and malonate ligands to provide some conformational rigidity to the optimized species. A number of stereoisomers were examined, and species **5**, a

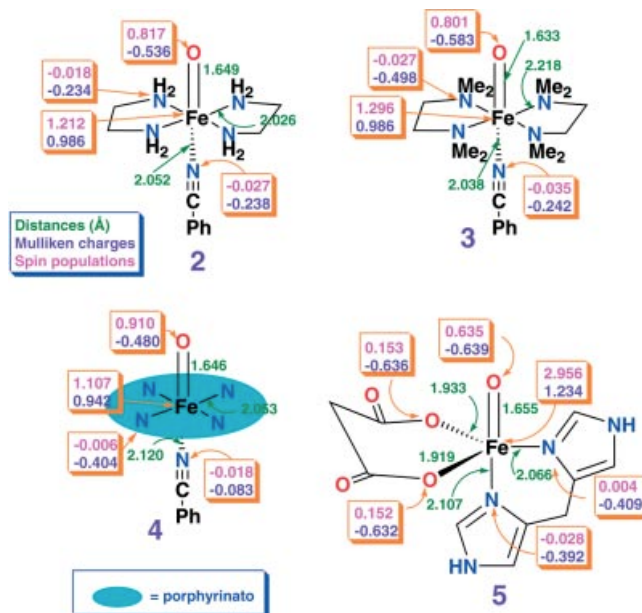


Figure 2. Selected optimized distances, Mulliken charges and spin populations for Fe<sup>IV</sup>O model complexes **2–5**; complexes **2–4** are  $S = 1$ , while **5** is  $S = 2$ .

five-coordinate trigonal-bipyramidal species shown in Figure 1, was found to have the lowest energy. Perhaps not surprisingly in view of its trigonal-bipyramidal structure, an  $S = 2$  spin state was favored over lower-spin states by several tenths of an eV. As shown in Figure 1, the Fe–O distance and O spin population for **5** are strikingly similar to those for the low-spin species **2–4**, indicating that the low-versus high-spin character of the Fe<sup>IV</sup>O unit has relatively little effect on the Fe( $d_{\pi}$ )–O( $p_{\pi}$ ) orbital interactions (which are largely responsible for the oxygen spin populations).

A comparison of the spin density profiles of **5** and of the Collins model complex **1** proved enlightening. If we define the Fe=O axis of **5** and the FeCl axis of **1** as the  $z$  direction, simple crystal field theory arguments (which are confirmed by our calculations) suggest that **5** should have a  $d_{z^2}$  hole, while **1** should have a  $d_{x^2-y^2}$  hole. Thus, if we describe the local symmetries of the iron centers in **5** and **1** as approximately  $C_{3v}$  and  $C_{4v}$ , then their ground states may be described as  $^5A_1$  and  $^5B_2$ , respectively. Further, we have already seen that the spin density profile of **5** is strongly affected by Fe( $d_{\pi}$ )–O( $p_{\pi}$ ) orbital interactions, for which there is no analogue in **1**. These considerations suggest that species **5** and **1** should exhibit significantly different spin density profiles, an expectation that is confirmed by Figure 3, which plots the spin density profiles for the two species. This may be seen as qualitatively consistent with the fact that the TauD intermediate and Collins' complex exhibit dramatically different Mössbauer spectroscopic parameters,<sup>[3,8]</sup> although these remain to be explicitly determined with DFT calculations.

Without question, the discovery of a high-spin Fe<sup>IV</sup> intermediate for TauD has galvanized biochemists and synthetic chemists alike to seek additional nonheme Fe<sup>IV</sup>O intermedi-



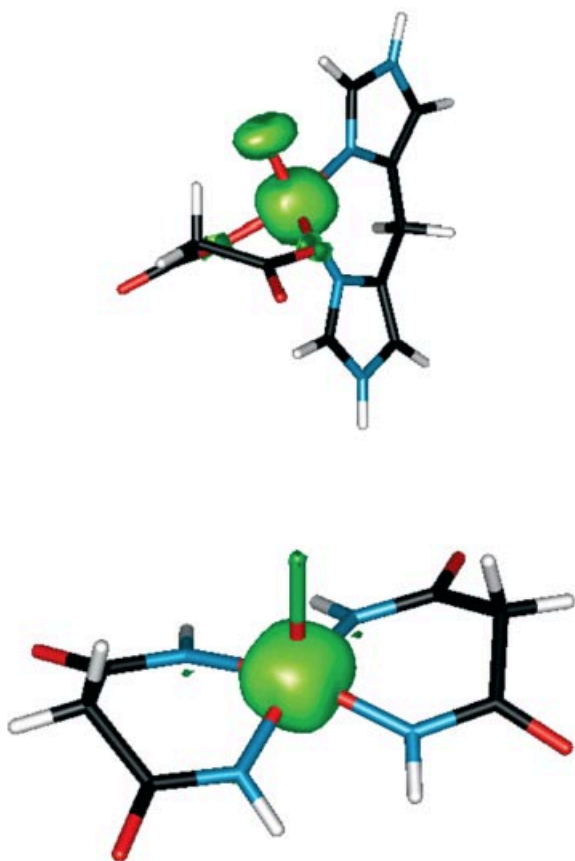


Figure 3. Comparison of the spin density profile of **5** (top) with that of a model (**1**, bottom) of Collins'  $S = 2$   $\text{Fe}^{\text{IV}}$  complex,  $[\text{Fe}^{\text{IV}}(\text{pmd-}N,N)_2\text{Cl}]^-$  (pmd- $N,N$  = propanediamidato- $N,N$ ); color code for atoms: calcd. C black, N blue, O red, H grey/white, and Cl green

ates. What might be a good strategy for the synthetic chemist? As alluded to above,<sup>[6,7,23,24]</sup> the use of 6-alkylated tpa ligands seems like a promising strategy, which led us to carry out geometry optimizations for both  $S = 1$  and  $S = 2$  states for the following four species:  $[\text{Fe}^{\text{IV}}(\text{O})(\text{X})(\text{Y})]^+$ , where  $\text{X} = \text{tpa}$  and 6- $\text{me}_3\text{-tpa}$  and  $\text{Y} = \text{F}$  and  $\text{OH}$  (Figure 4). Table 2 lists key geometry parameters and atomic spin populations, but these essentially lead to the same generalizations as made above for **2–5**, namely that the  $\text{Fe–O}$  distance and the O spin population are rather similar across all the species studied, regardless of spin state.

Table 2 shows that the PW91 calculations predict  $S = 1$  ground states for  $[\text{Fe}^{\text{IV}}(\text{O})(\text{tpa})(\text{Y})]^+$ , consistent with the experiment, but the preference for  $S = 2$  ground states for  $[\text{Fe}^{\text{IV}}(\text{O})(6\text{-me}_3\text{-tpa})(\text{Y})]^+$  is less clear. The B3LYP calculations clearly favor  $S = 2$  ground states for  $[\text{Fe}^{\text{IV}}(\text{O})(6\text{-me}_3\text{-tpa})(\text{OH})]^+$ , but also for  $[\text{Fe}^{\text{IV}}(\text{O})(\text{tpa})(\text{OH})]^+$ , albeit by a very slight margin. Elsewhere, we have documented that PW91 calculations exhibit a greater preference for low-spin states than B3LYP results.<sup>[10]</sup> Thus, at least certain of these calculations deserve to be repeated with more definitive but far more computationally demanding CASPT2 calculations. These uncertainties notwithstanding, the energetics

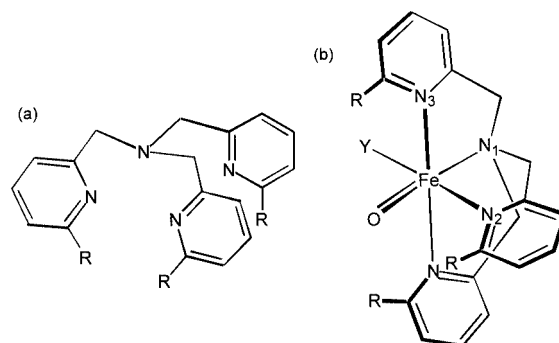


Figure 4. (a) Ligands used in calculations summarized in Table 2; tpa,  $\text{R} = \text{H}$ , 6- $\text{me}_3\text{-tpa}$ ,  $\text{R} = \text{CH}_3$ ; (b) note the notation of the  $\text{N}_1$ ,  $\text{N}_2$ ,  $\text{N}_3$  and  $\text{Y}$  atoms/groups, which are mentioned in Table 2

data shown in Table 1 suggest that there is a good chance that  $[\text{Fe}^{\text{IV}}(\text{O})(6\text{-me}_3\text{-tpa})(\text{Y})]^+$  species may exhibit  $S = 2$  ground states and, therefore, are attractive targets for synthetic modeling studies.

Finally, we have examined the question of whether Que's "flexible diamond core" may be viewed as one containing a high-spin  $\text{Fe}^{\text{IV}}=\text{O}$  unit.<sup>[22]</sup> For simplicity, we have only studied the ferromagnetically coupled  $S = 9/2$  state of the  $[(6\text{-me}_3\text{-tpa})\text{Fe}^{\text{III}}(\mu\text{-O})_2\text{Fe}^{\text{IV}}(6\text{-me}_3\text{-tpa})]^{3+}$  cation. The calculation employed a diamond-core-like starting geometry but only a  $C_s$  symmetry constraint to allow for spontaneous desymmetrization of the  $\text{Fe}_2(\mu\text{-O})_2$  core, which indeed took place;<sup>[28]</sup> selected geometry parameters and Mulliken spin populations for the two spin states are shown in Figure 5.

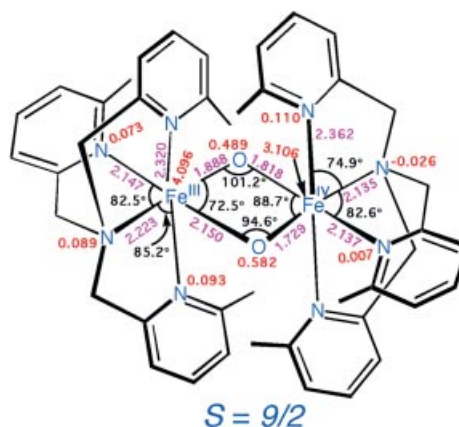


Figure 5. Selected PW91/TZP optimized distances (Å, magenta), angles (°, black) and Mulliken spin populations (red) for the ferromagnetically coupled  $S = 9/2$  state of the  $[(6\text{-me}_3\text{-tpa})\text{Fe}^{\text{III}}(\mu\text{-O})_2\text{Fe}^{\text{IV}}(6\text{-me}_3\text{-tpa})]^{3+}$  cation

The geometrical asymmetry of the  $\text{Fe}_2\text{O}_2$  unit (which seems consistent with its flexible nature, as emphasized in the experimental study<sup>[22]</sup>) and the spin density profile clearly indicate the presence of localized high-spin  $\text{Fe}^{\text{III}}$  and  $\text{Fe}^{\text{IV}}$  centers for both spin states. Thus, the  $\text{Fe}^{\text{IV}}$  center has a short  $\text{Fe–O}$  bond of about 1.73 Å, consistent with a high-spin  $\text{Fe}^{\text{IV}}=\text{O}$  unit. Note that the nitrogen atom *trans* to this

Table 2. Selected results on mononuclear tpa and 6-me<sub>3</sub>-tpa complexes: distances (Å), Mulliken spin populations, and relative energies ( $E_{\text{rel}}$ , eV); in general, the results refer to PW91/TZP calculations, while those shown in italics refer to single-point B3LYP/6-311G(d,p) calculations on PW91/TZP optimized geometries

Compound	S	Distances					Mulliken spin populations						$E_{\text{rel}}$
		FeO	FeL	FeN	FeN <sub>2</sub>	FeN <sub>3</sub>	Fe	O	Y	N <sub>1</sub>	N <sub>2</sub>	N <sub>3</sub>	
[(tpa)Fe(O)(F)] <sup>+</sup>	1	1.65	1.84	2.13	2.00	1.98	1.26	0.79	0.01	−0.01	−0.01	−0.01	0.00
[(tpa)Fe(O)(F)] <sup>+</sup>	2	1.65	1.81	2.19	2.09	2.24	2.97	0.66	0.15	−0.02	0.01	0.08	0.50
[(tpa)Fe(O)(OH)] <sup>+</sup>	1	1.65	1.90	2.15	2.03	1.98	1.29	0.78	−0.01	−0.01	0.00	−0.01	0.00
	<i>1</i>						<i>1.33</i>	<i>0.78</i>	<i>−0.03</i>				<i>0.00</i>
[(tpa)Fe(O)(OH)] <sup>+</sup>	2	1.65	1.83	2.26	2.09	2.26	2.88	0.68	0.25	−0.01	0.00	0.07	0.29
	<i>2</i>						<i>3.05</i>	<i>0.66</i>	<i>0.17</i>				<i>−0.07</i>
[(6-me <sub>3</sub> -tpa)Fe(O)(F)] <sup>+</sup>	1	1.65	1.85	2.10	2.08	2.08	1.24	0.79	0.00	−0.02	−0.00	−0.01	0.00
[(6-me <sub>3</sub> -tpa)Fe(O)(F)] <sup>+</sup>	2	1.64	1.82	2.14	2.16	2.32	2.97	0.67	0.14	−0.02	0.01	0.08	0.08
[(6-me <sub>3</sub> -tpa)Fe(O)(OH)] <sup>+</sup>	1	1.64	1.90	2.12	2.12	2.08	1.27	0.78	−0.03	−0.02	0.01	−0.01	0.12
	<i>1</i>						<i>1.35</i>	<i>0.76</i>	<i>−0.06</i>				<i>0.54</i>
[(6-me <sub>3</sub> -tpa)Fe(O)(OH)] <sup>+</sup>	2	1.65	1.84	2.18	2.16	2.37	2.89	0.70	0.24	−0.02	0.01	0.07	0.00
	<i>2</i>						<i>3.13</i>	<i>0.56</i>	<i>0.20</i>				<i>0.00</i>

group has a small negative spin population, unlike all the other nitrogen atoms, but consistent with the expectation that the metal  $d_{z^2}$  orbital that lies along the  $\text{Fe}^{\text{IV}}=\text{O}$  unit is formally unoccupied.

## Summary

The main conclusions of this study may be enumerated as follows.

(1) We began this study by an attempt to benchmark the relative energies of the high- and low-spin states for a well-characterized high-spin  $\text{Fe}^{\text{IV}}$  complex. Based on the CCSD(T) and CASPT2 results on model complex **1**, we would like to assert that the triplet-quintet splitting is likely to be larger than 0.3 eV and perhaps as large as 0.7 eV. Obviously, we wish we could have narrowed down this range somewhat, but that seems impossible with currently available technology. If this range is correct, then the DFT values are on the low side, consistent with the known tendency of DFT to favor low-spin states.<sup>[10]</sup> On a more positive note, DFT does not perform badly and does emerge as the practical tool of choice for a broad survey of high-spin  $\text{Fe}^{\text{IV}}$  species.

(2) The Fe–O distance and O spin population are quite similar across all mononuclear  $\text{Fe}^{\text{IV}}\text{O}$  species studied, regardless of the heme versus nonheme environment and of the  $S = 1$  versus 2 spin state, reflecting the essential similarity of the  $\text{Fe}(d_{\pi})-\text{O}(p_{\pi})$  orbital interactions in all these species.

(3) A significant insight from this study is that a high-spin  $\text{Fe}^{\text{IV}}$  center does not correspond to a unique type of electron spin density profile. Thus, the TauD intermediate and Collins' high-spin  $\text{Fe}^{\text{IV}}$  complex feature dramatically different spin density profiles, qualitatively consistent with their very different Mössbauer spectroscopic parameters.

(4) The sterically hindered 6-me<sub>3</sub>-tpa ligand and related ligands provide a promising recipe for generating synthetic  $S = 2 \text{Fe}^{\text{IV}}\text{O}$  intermediates.

(5) Lastly, our calculations indicate the presence of a fairly discrete high-spin  $\text{Fe}^{\text{IV}}=\text{O}$  unit in the mixed-valent, so-called “flexible diamond-core” intermediate.

**Supporting Information:** Optimized Cartesian coordinates for the different molecules studied are provided.

## Acknowledgments

This work was supported by a grant of computer time by the Research Council of Norway.

- [1] For a recent review, see: M. Costas, M. P. Mehn, M. P. Jensen, L. Que, Jr., *Chem. Rev.* **2004**, *104*, 939–986.
- [2] For a recent review, see: E. Y. Tshuva, S. J. Lippard, *Chem. Rev.* **2004**, *104*, 987–1011.
- [3] K. L. Kostka, B. G. Fox, M. P. Hendrich, T. J. Collins, C. E. F. Rickard, L. J. Wright, E. Münck, *J. Am. Chem. Soc.* **1993**, *115*, 6746–6757.
- [4] L. Shu, J. C. Nesheim, K. Kauffmann, E. Münck, J. D. Lipscomb, L. Que, Jr., *Science* **1997**, *275*, 515–518.
- [5] P. J. Riggs-Gelasco, L. Shu, S. Chen, D. Burdi, B. H. Huynh, L. Que, Jr., J. Stubbe, *J. Am. Chem. Soc.* **1998**, *120*, 849–860.
- [6] Y. Dong, L. Que, Jr., K. Kauffmann, E. Münck, *J. Am. Chem. Soc.* **1995**, *117*, 11377–11378.
- [7] H. Zheng, S. J. Yoo, E. Münck, L. Que, Jr., *J. Am. Chem. Soc.* **2000**, *122*, 3789–3790.
- [8] J. C. Price, E. W. Barr, B. Tirupati, J. M. Bollinger, Jr., C. Krebs, *Biochemistry* **2003**, *42*, 7497. Addition/Correction: *Biochemistry* **2004**, *43*, 1134–1134.
- [9] For a review, see: A. Ghosh, E. Steene, *J. Biol. Inorg. Chem.* **2001**, *6*, 739–752.
- [10] For a critical review of high-level ab initio calculations on systems of bioinorganic interest, see: A. Ghosh, P. R. Taylor, *Curr. Opin. Chem. Biol.* **2003**, *7*, 113–124.
- [11] Despite the popularity of DFT, the suitability of DFT for such unusual species as high-spin  $\text{Fe}^{\text{IV}}$  intermediates is hardly a foregone conclusion. Thus, DFT does not do a good job of pre-

- dicting the energy ordering of the low-lying spin states for some (porphyrin)Fe<sup>III</sup> derivatives: A. Ghosh, B. J. Persson, P. R. Taylor, *J. Biol. Inorg. Chem.* **2003**, *8*, 507–511.
- [12] The PW91 calculations were carried out using the ADF program system, using Slater-type TZP basis sets and a fine mesh for numerical integration of matrix elements. The B3LYP calculations were carried out using the program Turbomole and Gaussian basis sets of TZP quality. Adequately tight convergence criteria for geometry optimizations were used in all the calculations.
- [13] For the CASPT2 calculations, the CASSCF active space comprised eight electrons in eight orbitals: the five Fe 3d orbitals and three equatorial ligand orbitals, including two of  $a_1$  symmetry and one of  $a_2$ . The  $a_1$  symmetry equatorial ligand orbitals would be the  $\pi$  HOMO and LUMO if the ligands were exactly planar. The  $a_2$  symmetry ligand orbital is a combination of the N lone-pairs. The CASPT2 calculations were performed using the program Molcas 5.2 and the CCSD(T) calculations with Molpro 2002.
- [14] BS1 consisted of Dunning's cc-pVDZ basis sets on C, N O, and H, the aug-cc-pVDZ basis on Cl (T. H. Dunning, *J. Chem. Phys.* **1989**, *90*, 1007–1023), and a [6s5p4d3f2g] atomic natural orbital (ANO) basis on Fe (B. J. Persson, P. R. Taylor, unpublished results). BS2 consisted of Dunning's cc-pVTZ basis sets on C, N O, and H, the aug-cc-pVTZ basis on Cl (T. H. Dunning, *J. Chem. Phys.* **1989**, *90*, 1007–1023), and a [7s6p5d4f3g] ANO basis on Fe (B. J. Persson, P. R. Taylor, unpublished results). The Fe ANO basis sets are optimized for calculations that include Fe 3s3p correlation, the effects of which are not negligible here.
- [15] At present, there is extensive evidence (see, for example: P. E. M. Siegbahn, M. R. A. Blomberg, *Chem. Rev.* **2000**, *100*, 421–437) that DFT provides generally good results for geometries, spin density profiles, and a variety of other molecular properties for transition metal complexes. We believe that this generalization also holds for the species studied here and therefore largely refrain from commenting on the data presented in Table 1. However, one point worth noting is the relatively small amounts of spin density on the equatorial ligand set. By this criterion, the ligands may be described as relatively innocent, even though they must be extremely  $\sigma$ -donating.
- [16] For a discussion of population analyses, see: C. J. Cramer; *Essentials of Computational Chemistry: Theories and Models*, Wiley, Hoboken, NJ, USA, **2002**, pp. 278–291.
- [17] A few more technical comments may be worthwhile. Examining the CASSCF and CASPT2 results suggests that the wavefunctions for both states are somewhat multiconfigurational in character, but not exceptionally so. In this situation we would typically expect much closer agreement between CASPT2 and CCSD(T). We know that DFT (certainly with the functionals used here) tends to favour low-spin states; CASPT2 in its simplest implementation also tends to favour low-spin states but here we have used a modified Hamiltonian which gives a much better balanced treatment of different spin states, with no obvious preference for high or low spin. The 8-in-8 CASSCF/BS1 calculation itself gives 0.69 eV for the splitting (quintet lower), whereas a Hartree–Fock calculation gives 2.16 eV, again with the quintet lower. From the Hartree–Fock value we infer that electron correlation makes a substantial contribution to the splitting, which is expected; from the CASSCF value we can infer further that much of this correlation contribution is non-dynamical correlation. We must also recognize that the basis sets used here for the CCSD(T) calculations, though large, are far from complete and the contribution of dynamical correlation may well be larger in a more complete basis set.
- [18] C. A. Grapperhaus, B. Mienert, E. Bill, T. Weyhermüller, K. Wieghardt, *Inorg. Chem.* **2000**, *39*, 5306–5317.
- [19] M. H. Lim, J.-W. Rohde, A. Stubna, M. R. Bukowski, M. Costas, R. Y. N. Ho, E. Münck, W. Nam, L. Que, Jr., *Proc. Natl. Acad. Sci. U. S. A.* **2003**, *100*, 3665–3670.
- [20] J. Kaizer, E. J. Klinker, N. Y. Oh, J.-U. Rohde, W. J. Song, A. Stubna, J. Kim, E. Munck, W. Nam, L. Que, Jr., *J. Am. Chem. Soc.* **2004**, *126*, 472–473.
- [21] J.-W. Rohde, J.-H. In, M. H. Lim, W. W. Brennessel, M. R. Bukowski, A. Stubna, E. Münck, W. Nam, L. Que, Jr., *Science* **2003**, *299*, 1037–1039.
- [22] H. Zheng, S. J. Yoo, E. Münck, L. Que, Jr., *J. Am. Chem. Soc.* **2000**, *122*, 3789–3790.
- [23] Y. Zang, Y. Dong, L. Que, Jr., K. Kauffmann, E. Münck, *J. Am. Chem. Soc.* **1995**, *117*, 1169–1170.
- [24] Y. Zang, J. Kim, Y. Dong, E. C. Wilkinson, E. H. Appelman, L. Que, Jr., *J. Am. Chem. Soc.* **1997**, *119*, 4197–4205.
- [25] We used the PhCN ligand, instead of CH<sub>3</sub>CN, to exploit  $C_{2v}$  symmetry for species **2–4**.
- [26] See e. g. the first DFT calculation on an (porphyrin)Fe<sup>IV</sup>O: A. Ghosh, J. Almlöf, L. Que, Jr., *J. Phys. Chem.* **1994**, *98*, 5576–5579. The same effect (i. e. the complete localization of the spin density on the Fe and O atoms) was also noted in the first studies of high-valent iron diamond core intermediates A. Ghosh, J. Almlöf, L. Que, Jr., *Angew. Chem. Int. Ed. Engl.* **1996**, *35*, 770–772.
- [27] H. Kuramochi, L. Noodleman, D. A. Case, *J. Am. Chem. Soc.* **1997**, *119*, 11442–11451.
- [28] For a recent DFT study of valence-delocalized [Fe<sub>2</sub>( $\mu$ -O)<sub>2</sub>]<sup>3+,4+</sup> diamond-core species, see: A. Ghosh, E. Tangen, E. Gonzalez, L. Que, Jr., *Angew. Chem. Int. Ed.* **2004**, *43*, 834–838.

Received May 4, 2004

Early View Article

Published Online September 7, 2004